

available at www.sciencedirect.comjournal homepage: www.eu-openscience.europeanurology.com

European Association of Urology

Prostatic Disease

Comparison of Rotterdam and Barcelona Magnetic Resonance Imaging Risk Calculators for Predicting Clinically Significant Prostate Cancer

Juan Morote^{a,b,†,*}, Ángel Borque-Fernando^{c,†}, Marina Triquell^{a,b}, Miriam Campistol^{a,b}, Pol Servian^d, José M. Abascal^{e,f}, Jacques Planas^{a,b}, Olga Méndez^g, Luis M. Esteban^{h,‡}, Enrique Trilla^{a,b,‡}

^a Department of Urology, Vall d'Hebron Hospital, Barcelona, Spain; ^b Department of Surgery, Universitat Autònoma de Barcelona, Bellaterra, Spain; ^c Department of Urology, Hospital Miguel Servet, IIS-Aragon, Zaragoza, Spain; ^d Department of Urology, Hospital Germans Trias i Pujol, Badalona, Spain; ^e Department of Urology, Parc de Salut Mar, Barcelona, Spain; ^f Department of Surgery, Universitat Pompeu Fabra, Badalona, Spain; ^g Biomedical Research in Urology Unit, Vall d'Hebron Research Institute, Barcelona, Spain; ^h Department of Applied Mathematics, Escuela Universitaria Politécnica La Almunia, Universidad de Zaragoza, Zaragoza, Spain

Article info

Article history:

Accepted March 19, 2023

Associate Editor:

Guillaume Ploussard

Keywords:

Prostate cancer
Clinically significant
Early detection
Magnetic resonance imaging
Predictive model
Risk calculator

Abstract

Background: Magnetic resonance imaging (MRI)-based risk calculators (MRI-RCs) individualise the likelihood of clinically significant prostate cancer (csPCa) and improve candidate selection for prostate biopsy beyond the Prostate Imaging Reporting and Data System (PI-RADS).

Objective: To compare the Barcelona (BCN) and Rotterdam (ROT) MRI-RCs in an entire population and according to the PI-RADS categories.

Design, setting, and participants: A prospective comparison of BCN- and ROT-RC in 946 men with suspected prostate cancer in whom systematic biopsy was performed, as well as target biopsies of PI-RADS ≥ 3 lesions.

Outcome measurements and statistical analysis: Saved biopsies and undetected csPCa (grade group ≥ 2) were determined.

Results and limitations: The csPCa detection was 40.8%. The median risks of csPCa from BCN- and ROT-RC were, respectively, 67.1% and 25% in men with csPCa, whereas 10.5% and 3% in those without csPCa ($p < 0.001$). The areas under the curve were 0.856 and 0.844, respectively ($p = 0.116$). BCN-RC showed a higher net benefit and clinical utility over ROT-RC. Using appropriate thresholds, respectively, 75% and 80% of biopsies were needed to identify 50% of csPCa detected in men with PI-RADS < 3 , whereas 35% and 21% of biopsies were saved, missing 10% of csPCa detected in men with PI-RADS 3. BCN-RC saved 15% of biopsies, missing 2% of csPCa in men with PI-RADS 4, whereas ROT-RC saved 10%, missing 6%. No RC saved biopsies without missing csPCa in men with PI-RADS 5.

† These authors contributed equally as co-first authors.

‡ These authors contributed equally as co-last authors.

* Corresponding author. Department of Urology, Vall d'Hebron Hospital, Po Vall d'Hebron 119-129, 08035 Barcelona, Spain. Tel. +34 2746100; Fax: +34 2746028.

E-mail address: juan.morote@vallhebron.cat (J. Morote).

<https://doi.org/10.1016/j.euros.2023.03.013>

2666-1683/© 2023 The Author(s). Published by Elsevier B.V. on behalf of European Association of Urology. This is an open access article under the CC BY-NC-ND license (<http://creativecommons.org/licenses/by-nc-nd/4.0/>).



Conclusions: ROT-RC provided a lower and narrower range of csPCa probabilities than BCN-RC. BCN-RC showed a net benefit over ROT-RC in the entire population. However, BCN-RC was useful in men with PI-RADS 3 and 4, whereas ROT-RC was useful only in those with PI-RADS 3. No RC seemed to be helpful in men with negative MRI and PI-RADS 5.

Patient summary: Barcelona risk calculator was more helpful than Rotterdam risk calculator to select candidates for prostate biopsy.

© 2023 The Author(s). Published by Elsevier B.V. on behalf of European Association of Urology. This is an open access article under the CC BY-NC-ND license (<http://creativecommons.org/licenses/by-nc-nd/4.0/>).

1. Introduction

The early detection of prostate cancer (PCa) has evolved towards clinically significant PCa (csPCa), avoiding unnecessary prostate biopsies and overdiagnosis of insignificant tumours. However, PCa suspicion remains based on serum prostate-specific antigen (PSA) elevation and abnormal digital rectal examination (DRE) [1–3]. This paradigm shift has resulted from the spread of prebiopsy multiparametric magnetic resonance imaging (mpMRI), which grades the likelihood of csPCa through Prostate Imaging Reporting and Data System (PI-RADS) [4]. The negative predictive value of mpMRI reaches 95%, which makes it possible to avoid prostate biopsies for PI-RADS <3 [5,6]. Target biopsies of suspicious lesions (PI-RADS ≥ 3) increase the csPCa sensitivity of systematic-biopsies. However, csPCa detection does not exceed 20% in men with PI-RADS 3, is approximately 50% in men with PI-RADS 4, and reaches 90% in men with PI-RADS 5 [7].

MRI-predictive models individualise the likelihood of csPCa and improve candidate selection for prostate biopsy, although available risk calculators (RCs) and external validations are essential [8]. Among the 18 MRI-predictive models developed in the last 5 yr, seven have been validated externally and only two RCs are available [9]. Rotterdam (ROT) RC was initially designed from the Rotterdam population of the European Randomised Screening Prostate Cancer (ERSPC) trial [10,11]. ROT MRI-RC has resulted from an adjustment of the previous RCs 3 and 4 to predict PCa and high-grade PCa likelihoods in biopsy-naïve men and those with previous negative prostate biopsy, in 961 men with serum PSA ≥ 3.0 ng/ml and/or abnormal DRE, in whom systematic biopsy was always performed as a target biopsy to PI-RADSV.1 ≥ 3 lesions. PI-RADSV.1 score (1–5), age (50–75 yr), biopsy status (initial vs repeat), serum PSA (0.4–50 ng/ml), DRE (normal vs abnormal), and prostate volume (10–110 ml) were included as predictors [12]. ROT MRI-RC has been validated in some populations, although recalibrations and risk threshold adjustments have been needed to assure accurate predictions [13–16]. Barcelona (BCN) MRI-RC was recently designed among 1486 men with PSA ≥ 3.0 ng/ml and/or abnormal DRE, in whom systematic biopsies were always performed as target biopsies to PI-RADSV.2 ≥ 3 lesions. BCN MRI-RC has been validated externally and includes the same predictors as ROT MRI-RC without range limitation, PI-RADSV.2, and PCa family history (first degree vs no). The csPCa was defined as the Interna-

tional Society of Urologic Pathology (ISUP) grade group ≥ 2 . BCN MRI-RC has been the first predictive model analysed according to the PI-RADS categories, showing that the efficacy in the entire population does not represent that in each PI-RADS category. In addition, the BCN MRI-RC has the possibility to select the appropriate threshold for adjustments in validation studies and according to the PI-RADS categories [17].

Owing to differences between ROT and BCN MRI-RCs, we hypothesise different behaviour for improving candidate selection for prostate biopsy. We aim to compare the clinical usefulness of ROT and BCN MRI-RCs in a whole population of suspected PCa men and according to each PI-RADS category.

2. Patients and methods

2.1. Design, setting, and participants

A prospective head-to-head comparison of ROT- and BCN-RC in 946 men with serum PSA ≥ 3.0 ng/ml and/or abnormal DRE, recruited in two academic centres from the Barcelona metropolitan area (PSM and GTiP), between 2018 and 2021 was performed. Prebiopsy 3-Tesla mpMRI and 12-core transrectal ultrasound (TRUS) systematic biopsy were always performed, and two- to four-core TRUS visual target biopsies were added to PI-RADSV.2 ≥ 3 lesions. Men undergoing 5-ARIs who had previous PCa, atypical small acinar proliferation, or high-grade prostatic intraepithelial neoplasia with atypia were excluded. The project was approved by the ethical committee of VHH (PR/AG-317/2017).

2.2. Intervention

The likelihoods of csPCa from ROT-RC (www.prostatecancer-riskcalculator.com) [12] and BCN-RC (<https://mripcaprediction.shinyapps.io/MRIPCAPrediction/>, second tab 'BCN2RC: MRI-based model') [17] were assessed. PI-RADSV.2 was introduced in both RCs as the closest value of serum PSA, prostate volume, and age when out of the accepted range in ROT-RC.

2.3. Clinically significant PCa definition

ROT-RC predicts high-grade PCa likelihood, defined as a Gleason score of $\geq 3 + 4$, although the current RC shows this as csPCa [13]. BCN-RC predicts csPCa risk defined as an ISUP grade group of ≥ 2 [18].

2.4. Endpoint variables

Saved prostate biopsies and missed csPCa were determined.

2.5. Statistical analysis

Quantitative variables were expressed as median and 25–75 percentiles (interquartile range [IQR]), and qualitative variables in rates. Mann-Witney U test and chi-square test were used to compare medians and proportions [19,20]. The discrimination ability of csPCa was analysed with receiver operating characteristic (ROC) curves [21]; areas under the curve (AUCs) were compared with the test of DeLong et al [22]. Calibration curves analysed the correspondence between predictive probabilities and observed occurrence of csPCa. The net benefit of RCs over biopsying all men or none was analysed using a decision curve analysis (DCA) [23]. Specificities corresponding to 85%, 90%, and 95% sensitivities were assessed as their 95% confidence intervals (CIs). Clinical utility curves (CUCs) exploring potential rates of avoided biopsies and missed csPCa according to continuous probability of csPCa were generated [24]. Tests with two-sided $p < 0.05$ were considered statistically significant. Statistical analyses were computed using R programming language v.4.0.3 (The R Foundation for Statistical Computing, Vienna, Austria) and SPSS v.25 (Statistical Package for Social Sciences; IBM, San Francisco, CA, USA).

3. Results

3.1. Population characteristics

The characteristics of participants are summarised in Table 1. In 386 men (40.8%), csPCa was detected—17.9% in men with PI-RADS <3, 20.4% for PI-RADS 3, 51.9% for PI-RADS 4, and 84% for PI-RADS 5. A subset of 209 men (22.1%) had age (129), serum PSA (18), or prostate volume (68) out of the accepted range of ROT-RC.

3.2. Behaviour of ROT- and BCN-RC in the whole population

The median csPCa likelihood of ROT-RC was 3% (IQR: 2–10) in men without csPCa and 25% (9–46) in men with csPCa ($p < 0.001$), whereas those of BCN-RC were 10.5% (3.6–27.2) and 67.1% (39.3–85.6), respectively ($p < 0.001$; Fig. 1).

The calibration curves of both RCs showed certain underestimation of csPCa (Fig. 2A and 2B). BCN-RC showed a slight underestimation with a calibration in the large of 0.25 showing a minimum difference between the mean observed and the mean predicted values, with a difference of 1.96 for ROT-RC. The slopes were 0.81 and 1.04 for ROT- and BCN-RC, respectively. BCN-RC showed values near the ideal value of 1.

The discrimination ability of ROT- and BCN-RC for csPCa is presented by ROC curves in Figure 3A. The AUCs were 0.856 (95% CI: 0.831–0.881) and 0.844 (0.819–0.869) respectively ($p = 0.116$). BCN-RC showed a net benefit over biopsying all men from a 15% probability threshold; ROT MRI-RC showed the benefit from a 32% probability threshold (Fig. 3B). CUCs showed a larger clinical utility area for BCN-RC (Fig. 3C); additionally, the morphology and positioning of CUCs were different between the two RCs, shifted up and to the left of ROT-RC with respect to BCN-RC. The number of missed csPCa cases and avoided biopsies in each threshold from 1% to 100% are presented in Supplementary Table 1. The specificities corresponding to 85%, 90%, and 95% sensitivities of csPCa provided by both RCs are presented in Table 2. There were similar specificities at 85% and 90% sensitivities, with 42.1% (95% CI: 38.0–46.3) for

Table 1 – Population characteristics

Characteristic	Measurement
Number of men	946
Age (yr), median (IQR)	67 (61–72)
Total PSA (ng/ml), median (IQR)	7.4 (5.5–10.9)
Abnormal DRE, n (%)	307 (32.5)
Prostate volume (ml), median (IQR)	55 (40–79)
Prior negative prostate biopsy, n (%)	293 (31.0)
Family history of PCa, n (%)	34 (3.6%)
PI-RADS, n (%)	
1–2	235 (24.8)
3	201 (21.2)
4	391 (41.3)
5	119 (12.6)
PCa detection, n (%)	521 (55.1)
csPCa detection, n (%)	386 (40.8)
csPCa detection by PI-RADS category, n (%)	
<3	42 (17.9)
3	41 (20.4)
4	203 (51.9)
5	100 (84.0)

csPCa = clinically significant PCa; DRE = digital rectal examination; IQR = interquartile range; n = number; PCa = prostate cancer; PI-RADS = Prostate Imaging Reporting and Data System; PSA = prostate-specific antigen.

ROT-RC and 31.8% (28.0–35.8) for BCN-RC ($p < 0.001$) at 95% sensitivity.

3.3. Behaviour of ROT- and BCN-RC according to the PI-RADS categories

Violin plots of csPCa likelihoods in men with and without csPCa, assessed with both RCs according to PI-RADSV2 categories, show lower values and a narrow range of ROT-RC predictions (Fig. 4A) than those from BCN-RC (Fig. 4B), although significant differences existed between the medians of both subsets in all PI-RADS categories.

The AUC of ROT-RC in men with PI-RADS <3 was 0.776 (95% CI: 0.661–0.832), whereas the AUC of BCN-RC was 0.774 (0.697–0.850, $p = 0.529$; Fig. 5A). The AUCs were, respectively, 0.836 (0.756–0.916) and 0.838 (0.761–0.914) in men with PI-RADS 3 ($p = 0.954$; Fig. 5D), 0.829 (0.789–0.869) and 0.737 (0.677–0.787) in men with PI-RADS 4 ($p < 0.001$; Fig. 5G), and 0.866 (0.785–0.948) and 0.822 (0.723–0.920) in men with PI-RADS 5 ($p = 0.323$; Fig. 5J).

A small benefit over no-biopsy men with PI-RADS <3 was observed in both RCs (Fig. 5B). A clear net benefit of BCN-RC was observed over biopsying all men with PI-RADS 3 from a 10% csPCa probability, with the benefit of ROT-RC being lower (Fig. 5E). In men with PI-RADS 4, BCN-RC showed a net benefit over biopsying all men from a 17% csPCa probability; however, ROT-RC showed a small benefit between 50% and 75% csPCa probability (Fig. 5H). In men with PI-RADS 5, BCN-RC showed a benefit over biopsy-all men from 38% probability of csPCa; ROT-RC exhibited a minimal benefit from the 83% csPCa probability (Fig. 5K).

CUCs showed a striking behaviour of both RCs. ROT-RC started in PI-RADS <3 with curves displaced up and to the left, evolving with the increase of the PI-RADS category towards the graph diagonal line; BCN-RC run through the entire area of the graph, evolving from the top left to the bottom right with an increase in the PI-RADS category. CUCs of BCN-RC showed clear clinical utility in PI-RADS 3 and 4. The number of missed csPCa cases and saved biopsies in

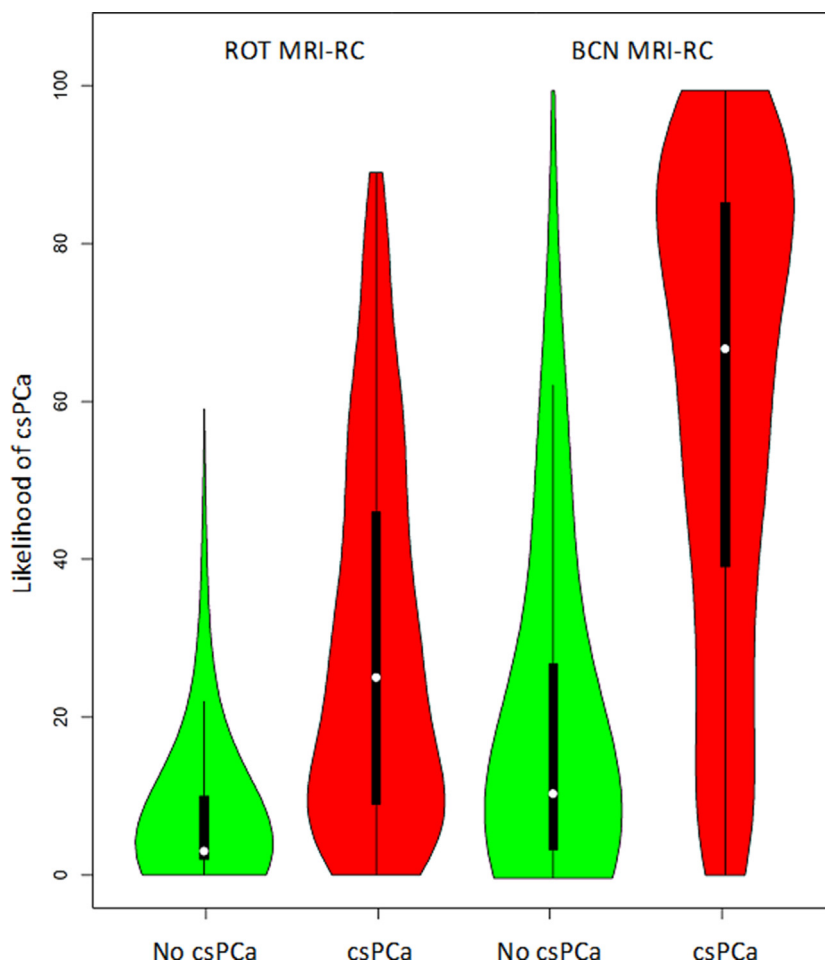


Fig. 1 – Violin plots of csPCA likelihoods of men without and with csPCA estimated with ROT MRI-RC and BCN MRI-RC. BCN = Barcelona; csPCA = clinically significant prostate cancer; MRI-RC = magnetic resonance imaging–based risk calculator; ROT = Rotterdam.

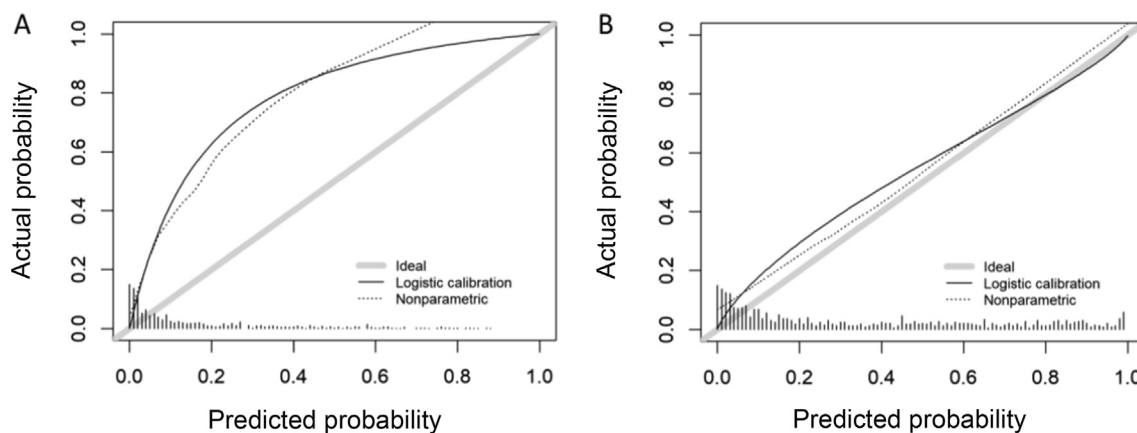


Fig. 2 – Calibration curves of (A) ROT MRI-RC and (B) BCN MRI-RC. BCN = Barcelona; MRI-RC = magnetic resonance imaging–based risk calculator; ROT = Rotterdam.

each PI-RADS category of ROT- and BCN-RC are presented in [Supplementary Tables 2–5](#). The specificities of both RCs from 85%, 90%, and 95% sensitivities in each PI-RADS category are presented in [Table 3](#).

As the decision of prostate biopsy is made after mpMRI, it is appropriate to define the acceptable percentages of

missed csPCA according to each PI-RADS category [17]. CUCs show how no RC appeared clinically helpful for PI-RADS <3 because, to identify 50% of 42 csPCA detected (5% of all csPCA detected), 75% of men needed biopsy (18.6% of all biopsies) with ROT-RC and 80% (20% of all biopsies) with BCN-RC. The rate of csPCA detection in men with PI-RADS

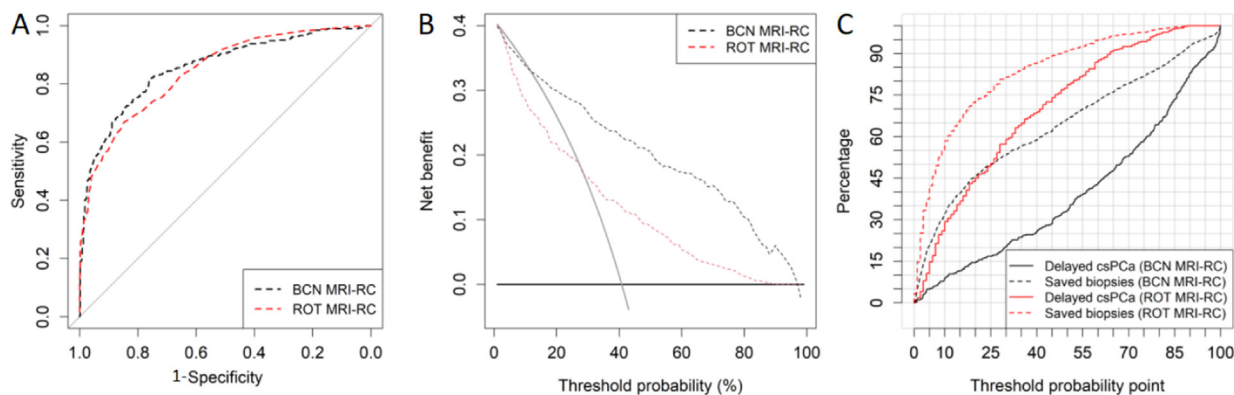


Fig. 3 – (A) Discrimination ability of csPCa of BCN MRI-RC and ROT MRI-RC presented with ROC curves, (B) net benefit of BCN MRI-RC and ROT MRI-RC over biopsying all men presented by DCAs, and (C) clinical utility of BCN MRI-RC and ROT MRI-RC showing the percentage of avoided biopsies and missed csPCa according to the threshold probability of csPCa by CUCs. BCN = Barcelona; csPCa = clinically significant prostate cancer; CUC = clinical utility curve; DCA = decision curve analysis; MRI-RC = magnetic resonance imaging–based risk calculator; ROT = Rotterdam.

Table 2 – Specificities of BCN MRI-RC and ROT MRI-RC corresponding to 85%, 90%, and 95% sensitivities for csPCa

Risk calculator	Specificity (95% CI) for sensitivities of					
	85%	<i>p</i> value	90%	<i>p</i> value	95%	<i>p</i> value
BCN MRI-RC (%)	67.3 (63.2–71.1)	0.055	52.0 (47.7–56.2)	0.392	31.8 (28.0–35.8)	<0.001
ROT MRI-RC (%)	61.7 (57.5–65.7)		54.7 (50.5–58.9)		42.1 (38.0–46.3)	

BCN = Barcelona; CI = confidence interval; MRI-RC = magnetic resonance imaging–based risk calculator; ROT = Rotterdam.

3 was 20.4%, and it was acceptable to miss up to 10% of these csPCa (5.2% of all csPCa) cases. ROT-RC saved 21% of biopsies, whereas BCN-RC saved 35%. In men with PI-RADS 4, BCN-RC saved 15% of biopsies (6% of all biopsies), missing 2% of csPCa (1% of all csPCa), whereas ROT-RC saved 10% of biopsies, with 6% of csPCa remaining undetected, which seems clinically unacceptable. Finally, in PI-RADS 5 where only 16% of biopsies were unnecessary, no RC assured to avoid any biopsy without missing csPCa.

4. Discussion

We were surprised at how far from the ideal was the calibration curve of ROT MRI-RC compared with that of BCN MRI-RC. The most probable cause was the low and narrow csPCa risk prediction range generated by ROT-RC mainly located at low predicted probabilities. We also noted that 22.1% of analysed suspected PCa men showed age, serum PSA, or prostate volume out of the accepted range of ROT MRI-RC. This drawback, not reported until now, can be a consequence of the strict inclusion criteria of the ERSPC trial in which RCs 3 and 4 were initially developed [10,11]. These limited ranges were not observed in the population of suspected PCa men in whom the ROT MRI-RC was adjusted [12], which had similar characteristics as our population study [17].

The discrimination ability of csPCa of ROT and BCN MRI-RCs was similar in the entire population; however, DCAs showed a net benefit of BCN MRI-RC over ROT MRI-RC. Since three-quarters of csPCa likelihoods predicted by ROT MRI-RC were below 24%, there was no benefit over biopsying

all men from a threshold of >20%, and misclassification of csPCa > 60% remained within these thresholds that are not in the utility range [23]. In contrast, BCN MRI-RC showed a net benefit over biopsying all men above the 15% threshold. This threshold avoided 40% of prostate biopsies, missing 10% of csPCa. To know the true clinical value of MRI-RCs is essential to assess their behaviour according to the PI-RADS categories, because the discrimination ability in the whole population does not represent that of each PI-RADS [25]. ROT MRI-RC showed no benefit in men with PI-RADS <3, 4, and 5, as did BCN MRI-RC in PI-RADS <3 and 5. BCN MRI-RC showed a net benefit in men with PI-RADS 4, saving between 6% and 23% of prostate biopsies and missing between 1% and 5% of csPCa detected for risk thresholds between 13% and 28%. In men with PI-RADS 3, ROT MRI-RC with thresholds between 1% and 3% missed between 0% and 12% of csPCa, saving 0.5–45% of biopsies. BCN MRI-RC at thresholds between 1% and 11% missed between 0% and 12% csPCa, saving between 5% and 47% of biopsies.

The possible drawback of comparing both MRI-RCs in a population from the same metropolitan area where the BCN MRI-RC was developed, we note that csPCa detection rate in the cohort of suspected PCa men in whom ROT MRI-RC was adjusted was 35.8%, very close to that of 36.9% observed in the BCN MRI-RC development cohort [13,17]. The characteristics of participants of this head-to-head comparison were different from those of both the development and the adjustment cohorts of BCN and ROT MRI-RCs in terms of age, serum PSA, DRE, and csPCa detection rate of 40.8%. The close origin of this population to that of BCN MRI-RC development did not influence the results. Rather, we believe that the differences between BCN and

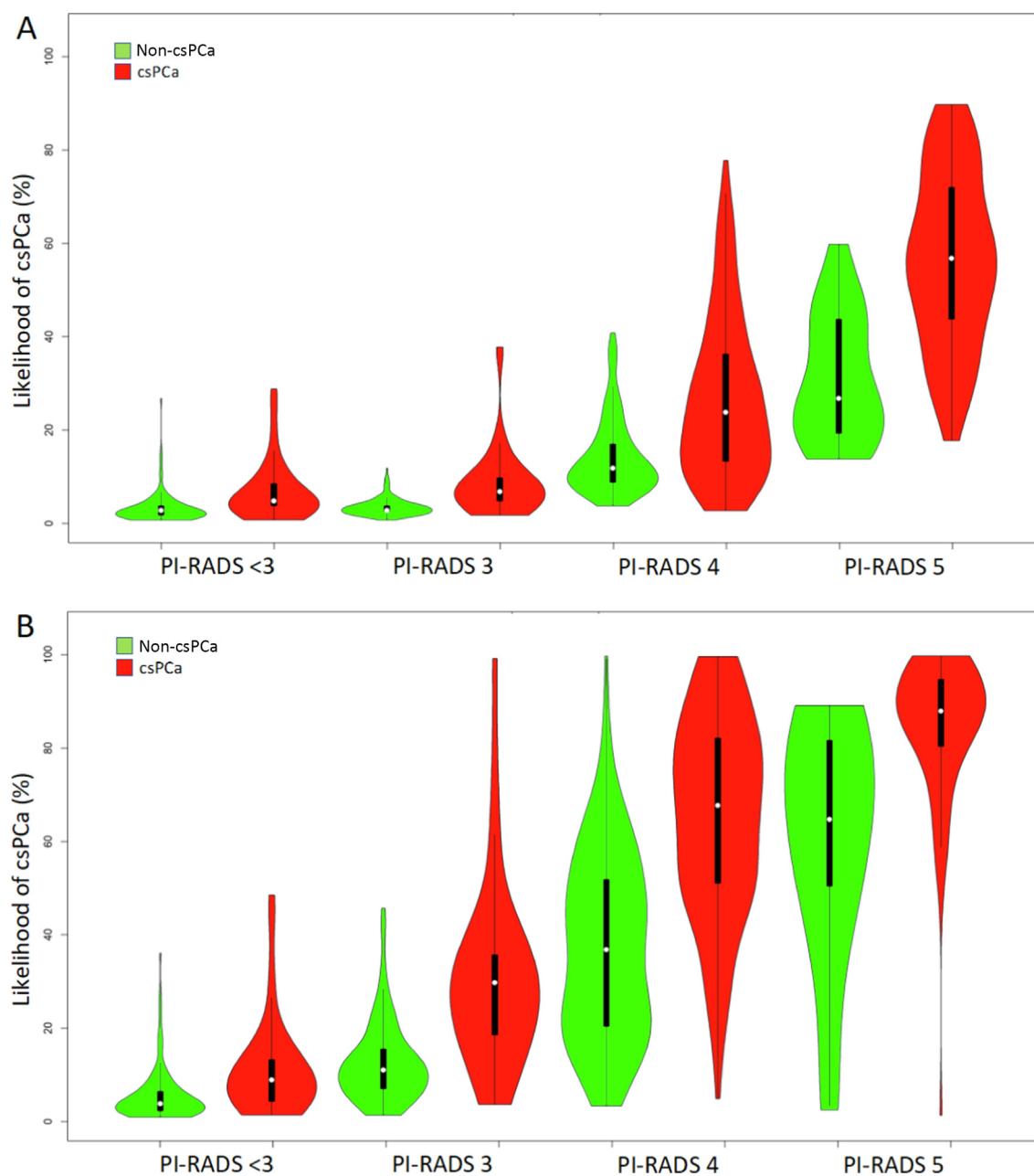


Fig. 4 – Violin plots of csPca likelihoods, estimated from (A) ROT MRI-RC and (B) BCN MRI-RC, in men without and with csPca according to the PI-RADS categories. BCN = Barcelona; csPca = clinically significant prostate cancer; MRI-RC = magnetic resonance imaging–based risk calculator; PI-RADS = Prostate Imaging Reporting and Data System; ROT = Rotterdam.

ROT MRI-RCs justify their different usefulness. BCN MRI-RC predicted the likelihood of csPca defined as grade group ≥ 2 , while ROT MRI-RC defined as Gleason $\geq 3 + 4$; the age, serum PSA, and prostate volume ranges were limited in ROT MRI-RC and PI-RADSV.1 was used in its adjustment cohort, whereas PI-RADSV.2 was used in the BCN MRI-RC development cohort. The expression of csPca likelihoods without and with decimals in ROT and BCN MRI-RCs, respectively, may represent any bias. A limitation of both MRI-RCs and the present study may be that a transperineal approach is currently recommended for prostate biopsy, whereas a transrectal approach was used in the present

ROT MRI-RC adjustment and BCN MRI-RC development comparative cohorts [1], which appears to improve the overall detection of csPca [26].

There are specific limitations of predictive models. A developed predictive model reflects the probability of a condition based on the characteristics at that time. However, changes arising in the same population and those from the validation cohorts justify the need of recalibrations of the models and adjustment of risk thresholds to ensure accurate predictions [27,28]. BCN MRI-RC reports the novelty of selecting the risk threshold that can be useful in external validations and selecting appropriate thresholds

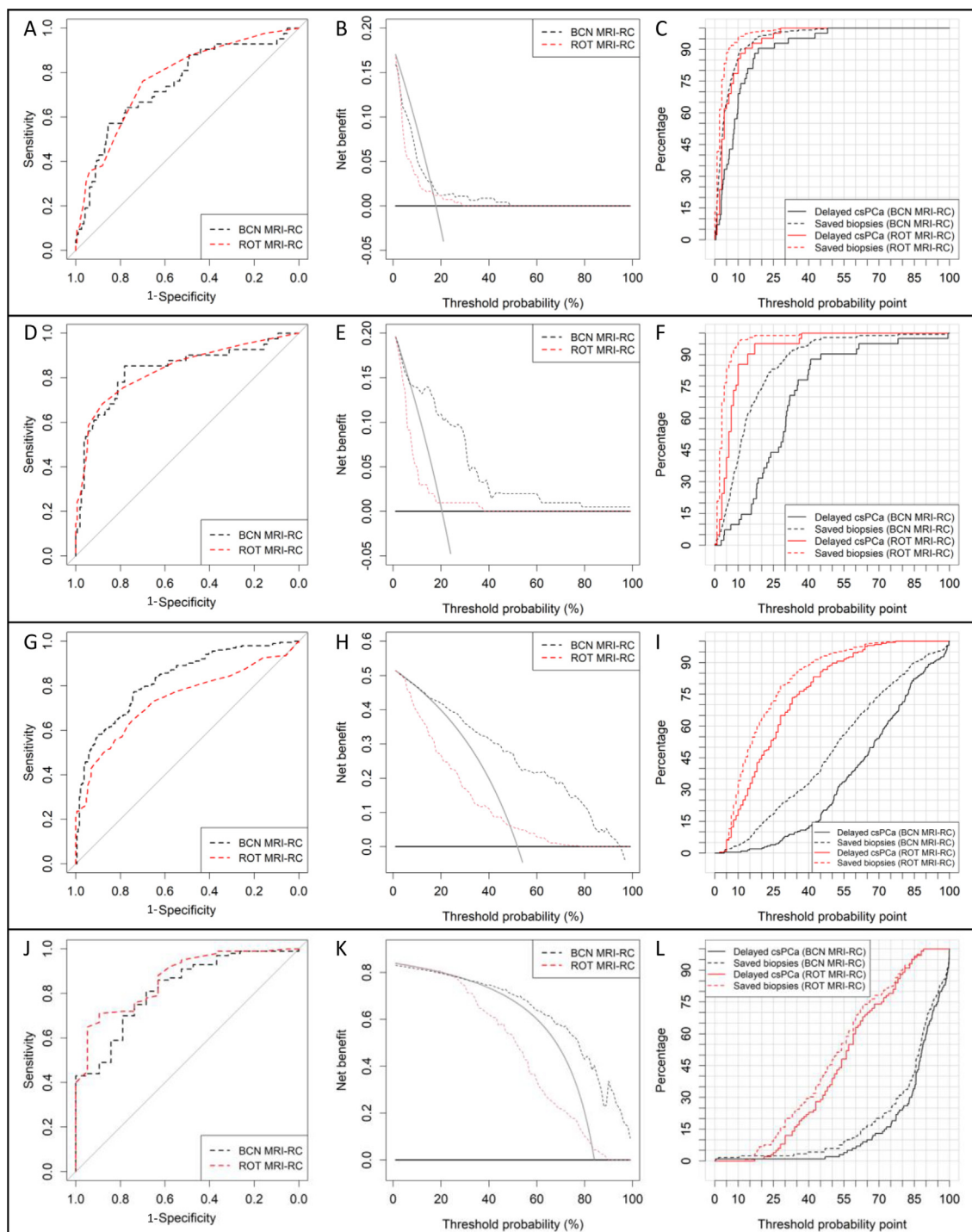


Fig. 5 – Discrimination ability presented by ROC curves, net benefit presented by DCAs, and clinical utility presented by CUCs, of BCN MRI-RC and ROT MRI-RC according to the PI-RADS categories: (A–C) PI-RADS <3, (D–F) PI-RADS 3, (G–I) PI-RADS 4, and (J–L) PI-RADS 5. BCN = Barcelona; csPca = clinically significant prostate cancer; CUC = clinical utility curve; MRI-RC = magnetic resonance imaging–based risk calculator; PI-RADS = Prostate Imaging Reporting and Data System; ROT = Rotterdam.

for each PI-RADS category [17]. Real-time updating is a great challenge for future RCs [29]. Continuous feedback of new cases, big data integration, appropriate machine learning algorithms, and federated networking can lead to future RCs validated in each site and ensuring accurate and long-lasting predictions in many places [30].

5. Conclusions

BCN and ROT MRI-RCs showed different behaviour in this head-to-head comparative analysis. ROT MRI-RC reported a lower and narrower range of csPca likelihoods than BCN MRI-RC. BCN MRI-RC presented a net benefit over ROT

Table 3 – Specificities of BCN MRI-RC and ROT MRI-RC corresponding to 85%, 90%, and 95% sensitivities for csPca according to the PI-RADSv2 category

Risk calculator	Specificity (95% CI) for sensitivities of					
	85%	p value	90%	p value	95%	p value
BCN MRI-RC (%)	49.7 (45.5–54.0)	0.188	PI-RADS <3 44.0 (39.9–48.3)	0.456	9.8 (7.6–12.7)	<0.001
ROT MRI-RC (%)	53.8 (49.6–58.0)		41.7 (37.6–45.9)		24.5 (21.1–28.3)	
BCN MRI-RC (%)	78.1 (74.4–81.4)	<0.001	PI-RADS 3 50.6 (46.4–54.8)	0.102	15.6 (12.8–19.0)	<0.001
ROT MRI-RC (%)	60.0 (55.8–64.0)		45.6 (41.4–49.8)		25.5 (22.0–29.4)	
BCN MRI-RC (%)	62.2 (58.1–66.2)	<0.001	PI-RADS 4 49.5 (45.3–53.7)	<0.001	39.9 (32.9–41.0)	<0.001
ROT MRI-RC (%)	29.7 (26.0–33.7)		20.2 (17.0–23.8)		4.6 (3.1–6.8)	
BCN MRI-RC (%)	63.2 (59.0–67.1)	1.000	PI-RADS 5 52.6 (48.4–56.8)	0.456	36.8 (32.9–41.0)	<0.001
ROT MRI-RC (%)	63.2 (59.0–67.1)		60.5 (56.3–64.6)		52.6 (48.4–56.8)	

BCN = Barcelona; CI = confidence interval; MRI-RC = magnetic resonance imaging–based risk calculator; PI-RADS = Prostate Imaging Reporting and Data System; ROT = Rotterdam.

MRI-RC and greater clinical utility in the entire population. According to the PI-RADS category, BCN MRI-RC was helpful in men with PI-RADS 3 and 4, whereas ROT MRI-RC was helpful only in men with PI-RADS 3. No MRI-RC was helpful in men with PI-RADS <3 and 5.

Author contributions: Juan Morote had full access to all the data in the study and takes responsibility for the integrity of the data and the accuracy of the data analysis.

Study concept and design: Morote, Borque-Fernando, Esteban.

Acquisition of data: Triquell, Campistol, Servian, Abascal, Mendez, Planas.

Analysis and interpretation of data: Morote, Borque-Fernando, Esteban.

Drafting of the manuscript: Morote.

Critical revision of the manuscript for important intellectual content:

Borque-Fernando, Esteban, Planas, Mendez, Trilla.

Statistical analysis: Esteban, Borque-Fernando, Morote.

Obtaining funding: Morote.

Administrative, technical, or material support: Morote.

Supervision: Morote, Trilla.

Other: None.

Financial disclosures: Juan Morote certifies that all conflicts of interest, including specific financial interests and relationships and affiliations relevant to the subject matter or materials discussed in the manuscript (eg, employment/affiliation, grants or funding, consultancies, honoraria, stock ownership or options, expert testimony, royalties, or patents filed, received, or pending), are the following: None.

Funding/Support and role of the sponsor: This study was supported by the Instituto Carlos III (SP) and the European Union (project ref: PI20/01666).

Appendix A. Supplementary data

Supplementary data to this article can be found online at <https://doi.org/10.1016/j.euros.2023.03.013>.

References

[1] Mottet N, van den Bergh RCN, Briers E, et al. EAU-EANM-ESTRO-ESUR-SIOG guidelines on prostate cancer—2020 update. Part 1:

screening, diagnosis, and local treatment with curative intent. *Eur Urol* 2021;79:243–62.

- [2] Van Poppel H, Roobol MJ, Chapple CR, et al. Prostate-specific antigen testing as part of a risk-adapted early detection strategy for prostate cancer: European Association of Urology position and recommendations for 2021. *Eur Urol* 2021;80:703–11.
- [3] Van Poppel H, Hogenhout R, Albers P, van den Bergh RCN, Barentsz JO, Roobol MJ. European model for an organised risk-stratified early detection programme for prostate cancer. *Eur Urol Oncol* 2021;10:731–9.
- [4] Schoots IG, Padhani AR, Rouvière O, Barentsz JO, Richenberg J. Analysis of magnetic resonance imaging-directed biopsy strategies for changing the paradigm of prostate cancer diagnosis. *Eur Urol Oncol* 2020;3:32–41.
- [5] Sathianathen NJ, Omer A, Harriss E, et al. Negative predictive value of multiparametric magnetic resonance imaging in the detection of clinically significant prostate cancer in the prostate imaging reporting and data system era: a systematic review and meta-analysis. *Eur Urol* 2020;78:402–14.
- [6] Wagaskar VG, Levy M, Ratnani P, et al. Clinical utility of negative multiparametric magnetic resonance imaging in the diagnosis of prostate cancer and clinically significant prostate cancer. *Eur Urol Open Sci* 2021;28:9–16.
- [7] Mazzone E, Stabile A, Pellegrino F, et al. Positive predictive value of Prostate Imaging Reporting and Data System version 2 for the detection of clinically significant prostate cancer: a systematic review and meta-analysis. *Eur Urol Oncol* 2020;4:697–713.
- [8] Osses DF, Roobol MJ, Schoots IG. Prediction medicine: biomarkers, risk calculators and magnetic resonance imaging as risk stratification tools in prostate cancer diagnosis. *Int J Mol Sci* 2020;20:1637.
- [9] Triquell M, Campistol M, Celma A, et al. Magnetic resonance imaging-based predictive models for clinically significant prostate cancer: a systematic review. *Cancers (Basel)* 2022;14:4747.
- [10] Steyberg R, Roobol-Bouts MJ, Kranse M, Schroder FH. Data storage device and method for determining the dependency of the risk for prostate cancer, device and method for indicating a risk for a disease in an individual. U.S. Patent Office, 8,087,576.
- [11] Roobol MJ, Steyberg EW, Kranse R, et al. A risk-based strategy improves prostate-specific antigen-driven detection of prostate cancer. *Eur Urol* 2010;57:79–85.
- [12] Alberts AR, Roobol MJ, Verbeek JFM, et al. Prediction of high-grade prostate cancer following multiparametric magnetic resonance imaging: improving the Rotterdam European Randomized Study of Screening for Prostate Cancer risk calculators. *Eur Urol* 2019;75:310–8.
- [13] Püllen L, Radtke JP, Wiesenfarth M, et al. External validation of novel magnetic resonance imaging-based models for prostate cancer prediction. *BJU Int* 2020;125:407–16.
- [14] Chen R, Verbeek JFM, Yang Y, Song Z, Sun Y, Roobol MJ. Comparing the prediction of prostate biopsy outcome using the Chinese Prostate Cancer Consortium (CPCC) risk calculator and the Asian adapted Rotterdam European Randomized Study of Screening for Prostate Cancer (ERSPC) risk calculator in Chinese and European men. *World J Urol* 2021;39:73–80.

- [15] Petersmann AL, Remmers S, Klein T, et al. External validation of two MRI-based risk calculators in prostate cancer diagnosis. *World J Urol* 2021;39:4109–16.
- [16] De Nunzio C, Lombardo R, Baldassarri V, et al. Rotterdam mobile phone app including MRI data for the prediction of prostate cancer: a multicenter external validation. *Eur J Surg Oncol* 2021;47:2640–5.
- [17] Morote J, Borque-Fernando A, Triquell M, et al. The Barcelona predictive model of clinically significant prostate cancer. *Cancers (Basel)* 2022;14:1589.
- [18] Epstein JI, Zelefsky MJ, Sjoberg DD, et al. A contemporary prostate cancer grading system: a validated alternative to the Gleason score. *Eur Urol* 2016;69:428–35.
- [19] Whitney J. Testing for differences with the nonparametric Mann-Whitney U test. *J. Wound Ostomy Continence Nurs* 1997;24:12.
- [20] Plackett RL. Karl Pearson and the chi-squared test. *Int Stat Rev* 1983;51:59–72.
- [21] Creelman CD, Donaldson W. ROC curves for discrimination of linear extent. *J Exp Psychol* 1968;77:514–6.
- [22] DeLong ER, DeLong DM, Clarke-Pearson DL. Comparing the areas under two or more correlated receiver operating characteristic curves: a nonparametric approach. *Biometrics* 1988;44:837–45.
- [23] Vickers AJ, Elkin EB. Decision curve analysis: a novel method for evaluating prediction models. *Med Decis Making* 2006;26:565–74.
- [24] Borque Á, Rubio-Briones J, Esteban LM, et al. Implementing the use of nomograms by choosing threshold points in predictive models: 2012 updated Partin tables vs a European predictive nomogram for organ-confined disease in prostate cancer. *BJU Int* 2014;113:878–86.
- [25] Moonesingh SR, Bashford T, Wagstaff D. Implementing risk calculators: time for the Trojan horse? *Anesth Analg* 2018;121:1192–6.
- [26] Zattoni F, Marra G, Kasivisvanathan V, et al. The detection of prostate cancer with magnetic resonance imaging-targeted prostate biopsies is superior with the transperineal vs the transrectal approach. A European Association of Urology-Young Academic Urologists Prostate Cancer Working Group multi-institutional study. *J Urol* 2022;208:830–7.
- [27] Morote J, Borque-Fernando Á, Triquell M, Esteban LM, Trilla E. The true utility of predictive models based on magnetic resonance imaging in selecting candidates for prostate biopsy. *Eur Urol Open Sci* 2022;42:40–1.
- [28] Diniz MA. Statistical methods for validation of predictive models. *J Nucl Cardiol* 2022;29:3248–55.
- [29] Strobl AN, Vickers AJ, Van Calster B, et al. Improving patient prostate cancer risk assessment: moving from static, globally-applied to dynamic, practice-specific risk calculators. *J Biomed Inform* 2015;56:87–93.
- [30] Nandi A, Xhafa F. A federated learning method for real-time emotion state classification from multi modal streaming. *Methods* 2022;204:340–4.